The Simplest Laser-Based Optoelectronic Oscillator: An Experimental and Theoretical Study

Géraud Russel Goune Chengui, Paul Woafo, and Yanne K. Chembo, *Senior Member, IEEE*

***Abstract*—We present a theoretical and experimental study of the most simple autonomous optoelectronic oscillator (OEO) with a delayed feedback loop. Contrarily to the overwhelming majority of OEOs, our OEO does not use an external intensity- or phase-modulator to translate the electrical radio-frequency signal into the optical domain. Instead, we show that the electric signal can simply be used as a driving pump current of the laser that is seeding the oscillator. With this architecture, the intensity modulation is performed through the piecewise-linear (that is, nonlinear) power-intensity transfer function of the laser-diode, instead of the sinusoidal transfer function of the usual Mach–Zehnder modulators. We provide a model to investigate the dynamics of this simple architecture of OEO. This model is an integro-differential delay equation which is characterized by three timescales as in the conventional OEO, namely the low/high-cutoff frequencies of the wideband filter and the time delay. The stability analysis of our OEO reveals a complex bifurcation behavior which critically depends on the gain of the feedback loop. In particular, we show that a sequence of Hopf bifurcations may lead to fast-scale oscillations with a period which is the double of the time-delay, or to slow-scale oscillations with a period which depends on the three aforementioned timescales. Our theoretical results are shown to be in excellent agreement with numerical simulations and the experimental measurements.**

***Index Terms*—Nonlinear oscillators, optoelectronic devices.**

I. Introduction

OPTOELECTRONIC OSCILLATORS (OEOs) are autonomous nonlinear systems whose feedback loop is constituted with an optical and an electrical branch. In the optical part, OEOs are seeded with a continuous-wave (cw) semiconductor laser (typically in the near-infrared range). The output laser beam is generally modulated using a nonlinear electro-optic modulator and subsequently launched into an optical fiber line which is long enough to induce a significant time delay. The optical beam is then converted into an electrical signal using a fast photodiode (PD). This radio-frequency (RF) signal is eventually bandpass or lowpass filtered, amplified, and then used as a driving signal of the modulator, thereby closing the feedback loop. Following this mechanism, OEOs can output RF signal with a frequency range from 1 kHz to 100 GHz, and they display a very wide range of complex dynamical behaviors.

These oscillators were initially investigated by Neyer and Voges [1], and they were rapidly identified as ideal experimental benchmarks to investigate some of the dynamical features of the paradigmatic Ikeda equation [2]. Many applications are related to OEOs, such as optical chaos cryptography and neuromorphic computing, for example (see review article [3] and references therein). However, the most well-known application is ultra-pure microwave generation for aerospace engineering applications, and this area of research was pioneered by Yao and Maleki in 1994, who are also those who coined the term OEO [4]–[6].

In most architectures of OEOs, the nonlinear conversion between the electrical and the optical signal is performed by a phase or an intensity modulator with sinusoidal transfer function. Models to investigate the dynamical properties of such architectures have been proposed for both the narrow-band [7]–[9] and wideband [10], [11] configurations of OEOs. However, it has been demonstrated that other electro-optic or optoelectronic devices can be used to perform this nonlinear conversion (see for instance [12]). The simplest example is to consider the seeding laser-diode (LD) itself as an electrical-to-optical converter through its power-intensity—or "PI"—transfer function. It is noteworthy that in the adiabatic limit (modulation frequency much slower than the relaxation frequency of the laser), the PI transfer function of a semiconductor laser is a "piece-wise linear" function equal to zero below a given threshold current I_{th}, and linearly increasing above. We therefore consider that this architecture corresponds to the simplest OEO possible, and it is relevant to perform a detailed theoretical and experimental study in order to understand its dynamical properties. Moreover, since this OEO does not require an electro-optic modulator (which is definitely one of the most expansive element of conventional OEOs), it appears to be a cost-effective alternative for frequency-versatile microwave generation.

The aim of this paper is to analyze this new OEO architecture where the LD nonlinearity is used to perform the conversion from the electrical to the optical domain. We show that the system displays a complex dynamics which depends on slow- and fast-scale limit-cycles that can arise in the system depending on the gain of the delayed feedback. We also successfully compare our analytical findings with numerical simulations and experimental measurements.

The outline of the paper is the following. The experimental system and the model governing the dynamics of the OEO are presented in Section II. We determine the fixed points and

Manuscript received July 27, 2015; revised November 7, 2015; accepted November 30, 2015. Date of publication December 16, 2015; date of current version February 5, 2016. This work was supported in part by the European Research Council through the project NextPhase (ERC StG 278616), by the *Centre National d'Etudes Spatiales* through the project SHYRO, by the *Région de Franche-Comté*, by the ANR project ORA, by the LabEx ACTION, and by the International Center for Theoretical Physics in Italy.

G. R. Goune Chengui and P. Woafo are with the Laboratory of Modelling and Simulation in Engineering, Biomimetics and Prototypes, Department of Physics, Faculty of Science, University of Yaoundé, Yaoundé, Cameroon (e-mail: geraud.goune@yahoo.fr; pwoafo1@yahoo.fr).

Y. K. Chembo is with the Optics Department, CNRS and University Bourgogne Franche-Comté, FEMTO-ST Institute, 25030 Besançon Cedex, France (e-mail: yanne.chembo@femto-st.fr).

Color versions of one or more of the figures in this paper are available online at http://ieeexplore.ieee.org.

Digital Object Identifier 10.1109/JLT.2015.2508784

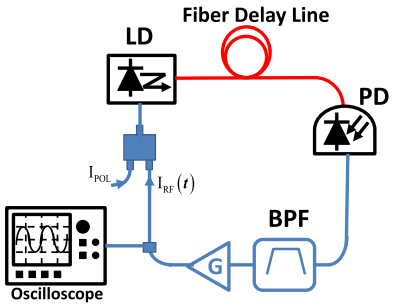

Fig. 1. Experimental set-up of the OEO. LD: Laser Diode; PD: Photo-Diode; G: Voltage Variable Attenuator (VVA); BPF: Band-Pass Filter.

analyze the bifurcation behavior of the oscillator in Section III. Numerical simulations are performed in Section IV, and compared with the experimental data. The last section concludes the article.

II. System and Model

Our OEO is displayed in Fig. 1 and it is constituted with several elements. The central element is the cw distributed feedback LD source with telecom wavelength $\lambda_{\rm L} = 1550$ nm. It has a threshold current $I_{\rm th} = 16$ mA, and it is driven by a pump current $I_{\rm pol} + I_{\rm RF}(t)$, where $I_{\rm pol}$ is the polarization current, while $I_{\rm RF}(t)$ is the time-varying RF current. The output of this LD has an output power $P(t)$ which can be varied from 0 to 10 mW. The optical fiber cable has a length $L = 40$ m, yielding a delay time $T = nL/c = 0.2$ μs where $n = 1.5$ is the refraction index of the fiber, and c is the velocity of light in vacuum. The optical signal is transformed into a photocurrent by an InGaAs PD with responsivity $S = 4.75$ V/mW at 1550 nm and detection bandwidth of 100 MHz. It is important to note that the wavelength variation with the laser pump current is $d\lambda_{\rm L}/dI = 0.5$ pm/mA at 1550 nm, so that the typical wavelength variation is of the order of 10 pm or less. This value is small enough for us to consider that the PD responsivity S is a constant. This PD converts the input power $P(t)$ into an electric voltage $V(t)$, which is applied to a voltage variable attenuator (VVA) with gain G (smaller than 1) and broadband bandwidth of 0.01–2.5 GHz. This voltage is converted back into a current $I_{\rm RF}(t)$, which is added to a polarization current $I_{\rm pol}$ using a Bias-Tee (0.1 MHz–2.2 GHz) before being used to pump the LD. The temperature of the laser was set to a constant value, but since we are only concerned with the deterministic dynamics of the system, the full oscillator was thermalized to the room temperature without any specific control.

The central element of our OEO is the LD, which seeds the optical branch of the oscillator and also performs the conversion from the electric to the optical domain. The dimensionless nonlinear transfer function of this LD is

$$\mathrm{D}(x) = x\,\mathrm{H}(x) = \begin{cases} 0, & \text{for } x \le 0 \\ x, & \text{for } x > 0 \end{cases} \tag{1}$$

where $\mathrm{H}(x)$ is the usual Heaviside step-function equal to 0 for $x \le 0$ and to 1 otherwise. The diode nonlinearity function $\mathrm{D}(x)$ is therefore null for negative x, and increases linearly when x is positive. In lasers, this diode function is usually of the form $\mu\,\mathrm{D}(I - I_{\rm th})$, which is equal to 0 for $I < I_{\rm th}$, and equal to $\mu(I - I_{\rm th})$ for $I \ge I_{\rm th}$. The parameter $\mu = \eta_d\, h\nu$ is the laser conversion slope, with η_d being the quantum efficiency, h the Planck constant, and $\nu = c/\lambda_{\rm L}$ the laser carrier frequency. We have experimentally determined that $\mu = 0.21$ mW/mA for our laser. The PI transfer function of our LD is therefore $P(t) = \mu\,\mathrm{D}[I_{\rm RF}(t) - I_0]$, that is

$$P(t) = \begin{cases} 0, & \text{for } I_{\rm RF}(t) \le I_0 \\ \mu[I_{\rm RF}(t) - I_0], & \text{for } I_{\rm RF}(t) > I_0 \end{cases} \tag{2}$$

where $I_0 = I_{\rm th} - I_{\rm pol}$. We expect the dynamics of our oscillator to be in the MHz range, that is, spectrally far below the relaxation oscillation of our LD which is in the GHz range. Therefore, even though the pump current and laser power are time dependent, it is legitimate to consider that the output power $P(t)$ adiabatically follows the pump current $I(t)$ via the nonlinear function D. Otherwise, if the system is allowed to oscillate at frequencies close to the GHz relaxation oscillation of the laser, the internal dynamics of the intra-cavity photon and carrier densities cannot be disregarded anymore and the system is known to display a large set of very complex nonlinear behaviors [13]–[18].

The dynamical properties of the system are ruled by the overall band-pass filtering induced by the superimposed bandwidths of the RF-amplifier, the PD and the coupler. We can take advantage of the fact that the low and high cut-off frequencies f_L and f_H are very distant one from each other, and consider that this band-pass filter is constituted of two cascaded high-pass and low-pass first order linear filters. The input voltage $V_{\rm in}(t)$ and output voltage $V_{\rm out}(t)$ of the cascaded band-pass filter are linked by the equation:

$$\left[1 + \frac{f_L}{f_H}\right] V_{\rm out}(t) + \frac{1}{2\pi f_H}\frac{dV_{\rm out}(t)}{dt} + 2\pi f_L \int_{t_0}^{t} V_{\rm out}(s)\,ds = V_{\rm in}(t). \tag{3}$$

The optical power P at the output of the optical fiber is converted into the electrical signal through the PD, according to the relation $V_{\rm in}(t) = SP(t - T)$, where T is the time delay originating from the propagation of the light beam in the fiber, and S is the responsivity of the PD. The input voltage of the electrical part circuit can therefore be written as $V_{\rm in}(t) = S\mu\,\mathrm{D}[I_{\rm RF}(t - T) - I_0]$. The relationship between $V_{\rm RF}(t)$ and the output voltage is $V_{\rm RF}(t) = \kappa G V_{\rm out}(t)$, where κ is a dimensionless factor standing for all the linear losses (electrical and optical) in the feedback loop. This voltage is converted into the current $I_{\rm RF}(t) = V_{\rm RF}(t)/R_Z$, where $R_Z = 50\,\Omega$ is characteristic impedance used for the voltage-to-intensity conversion. It can therefore be shown that the RF voltage $V_{\rm RF}(t)$ obeys the following equation:

$$\left[1 + \frac{f_L}{f_H}\right] V_{\rm RF}(t) + \frac{1}{2\pi f_H}\frac{dV_{\rm RF}(t)}{dt} + 2\pi f_L \int_{t_0}^{t} V_{\rm RF}(s)\,ds = \frac{\kappa S\mu G}{R_Z}\,\mathrm{D}[V_{\rm RF}(t - T) - V_0] \tag{4}$$

where V_0 is the equivalent intensity-to-voltage conversion of I_0 through $V_0 = R_Z I_0$. If we take $f_L \ll f_H$ into account, this equation can be rewritten under this simplified and dimensionless form

$$x(t) + \tau \frac{dx(t)}{dt} + \frac{1}{\theta}\int_{t_0}^{t} x(s)\,ds = \beta\,\mathrm{D}[x(t-T) - \alpha] \quad (5)$$

where the variable of the system is $x(t) = V_{\mathrm{RF}}(t)/V_{\mathrm{REF}}$, with with $V_{\mathrm{REF}} \equiv 1$ V being the reference voltage value (it is convenient in our case because it yields $|x(t)| = |V_{\mathrm{RF}}(t)|$). The parameters of Eq. (5) are the bandpass filter timescales $\tau = 1/2\pi f_H$ and $\theta = 1/2\pi f_L$, the offset dimensionless voltage $\alpha = V_0/V_{\mathrm{REF}}$, and the feedback loop gain $\beta = \kappa S \mu G/R_Z$. Equation (4) is a nonlinear integro-differential delay equation, which can be conveniently rewritten under the form

$$\dot{y} = x \quad (6)$$

$$\tau\dot{x} = -x - \frac{1}{\theta}y + \beta\,\mathrm{D}[x_T - \alpha] \quad (7)$$

where the overdot denotes the derivative with respect to time, $x_T \equiv x(t-T)$, and $y = \int_{t_0}^{t} x(s)\,ds$.

It should be noted that in our system, the bandpass filtering originates from cascaded elements of the loop. For numerical simulations, we will use the following parameter values which have been obtained from our experimental setup: $\tau = 25$ ns ($f_H = 6.4$ MHz), $\theta = 0.3\,\mu$s ($f_L = 531.5$ kHz), and $T = 0.2\,\mu$s (corresponding to 40 m of optical fiber).

III. Stability of the System

The linear stability analysis is based on analyzing the time-dependent trajectory of the system when slightly perturbed from the steady state $(x_{\mathrm{st}}; y_{\mathrm{st}})$. The flow of Eqs. (6) and (7) has a single stationary point which obeys:

$$\begin{aligned}(x_{\mathrm{st}}; y_{\mathrm{st}}) &= (0; \theta\beta\,\mathrm{D}[-\alpha]) \\ &= \begin{cases} (0; -\theta\beta\alpha), & \text{for } \alpha < 0 \\ (0;0), & \text{for } \alpha \geq 0. \end{cases}\end{aligned} \quad (8)$$

It is interesting to note that in all cases, the dimensionless voltage x_{st} is always null for the equilibria of the OEO, and this is due to the presence of the integral term in Eq. (5).

The solutions $x(t)$ and $y(t)$ can be represented as a sum of the steady state and a small perturbation following:

$$x(t) = x_{\mathrm{st}} + \delta x(t) \quad (9)$$

$$y(t) = y_{\mathrm{st}} + \delta y(t) \quad (10)$$

and inserting the preceding equations into Eqs. (6) and (7) leads to

$$\delta\dot{y} = \delta x \quad (11)$$

$$\tau\delta\dot{x} = -\delta x - \frac{1}{\theta}\delta y + \beta\,\mathrm{H}[-\alpha]\,\delta x_T \quad (12)$$

where we have assumed that the derivative of the nonlinear transfer function D is

$$\begin{aligned}\mathrm{D}'(x) &= \mathrm{H}(x) + x\,\mathrm{H}'(x) = \mathrm{H}(x) + x\,\delta(x) \\ &\equiv \mathrm{H}(x).\end{aligned} \quad (13)$$

From Eqs. (11) and (12), the stability of the system can be investigated after setting $\delta x, \delta y \propto e^{\lambda t}$, through the eigenvalue equation:

$$\tau\lambda^2 + \lambda\{1 - \beta e^{-\lambda T}\,\mathrm{H}[-\alpha]\} + \frac{1}{\theta} = 0 \quad (14)$$

and it appears that the stability of the system critically depends on the value of the dimensionless offset voltage α, and more specifically, on its sign.

A. Case $\alpha \geq 0$ (or $I_{\mathrm{pol}} \leq I_{\mathrm{th}}$)

In this case, the fixed point is the trivial equilibrium $(0;0)$, as shown in Eq. (8). Since $\mathrm{H}[-\alpha] \equiv 0$, the eigenvalue Eq. (14) becomes independent of the feedback gain parameter β and yields

$$\tau\lambda^2 + \lambda + \frac{1}{\theta} = 0 \quad (15)$$

with solutions

$$\lambda_{\pm} = \frac{1}{2\tau}\left[-1 \pm \sqrt{1 - 4\frac{\tau}{\theta}}\right]. \quad (16)$$

The above eigenvalues always have a strictly negative real part, regardless of the values of τ and θ. Therefore, in the case $\alpha \geq 0$, the fixed point $(0;0)$ is unconditionally stable, regardless of the value of the delay time T and feedback gain β. This result is interesting because this case $\alpha \geq 0$ corresponds to $I_{\mathrm{pol}} \leq I_{\mathrm{th}}$: it therefore appears that if the polarization current is smaller than the threshold current (and in particular, if $I_{\mathrm{pol}} = 0$), the system will remain in the trivial fixed point regardless of the gain and the time-delay. It also means that the polarization current is an absolutely necessary element in the system if one expects to obtain a non-trivial dynamical behavior.

B. Case $\alpha < 0$ (or $I_{\mathrm{pol}} > I_{\mathrm{th}}$)

In this case, the fixed point is $(0; -\theta\beta\alpha)$ according to Eq. (8). Hence, we have $\mathrm{H}[-\alpha] = 1$, and the eigenvalue Eq. (14) can be rewritten as

$$\tau\lambda^2 + \lambda\{1 - \beta e^{-\lambda T}\} + \frac{1}{\theta} = 0. \quad (17)$$

This nonlinear algebraic equation is transcendental and cannot be solved exactly. However, we know that Hopf bifurcations occur in the system when $\lambda = i\omega$, where ω is the angular frequency of the limit-cycles close to the bifurcation points. According to Eq. (17), the Hopf frequency ω necessarily obeys

$$\tau\omega^2 + \omega\beta\sin(\omega T) - \frac{1}{\theta} = 0 \quad (18)$$

$$\beta\cos(\omega T) - 1 = 0 \quad (19)$$

which can be transformed into

$$\omega\tan(\omega T) = -\tau\omega^2 + \frac{1}{\theta} \quad (20)$$

$$\beta^2 = 1 + \left[\frac{1}{\theta\omega} - \tau\omega\right]^2 \quad (21)$$

where Eq. (20) originates from the ratio between Eqs. (18) and (19), while Eq. (21) is obtained by the combination of the square of the same equations. Even though Eqs. (20) and (21) still cannot be solved exactly, pertinent simplifying assumptions can be made and enable us to find accurate analytical approximations for the first and second Hopf bifurcations.

The first bifurcation with the frequency ω_1 is obtained from the resolution of Eqs. (20) and (21) when we assume $\tan(\omega_1 T) \simeq 0$. The trivial solution $\omega_1 T \simeq 2\pi$ is obtained and then introduced into Eq. (21) in order to obtain β_1. The critical frequency and gain values at the Hopf bifurcation are therefore:

$$\omega_1 \simeq \frac{2\pi}{T} \tag{22}$$

$$\beta_1 \simeq \left[1 + \left(\frac{T}{2\pi\theta} - \frac{2\pi\tau}{T}\right)^2\right]^{\frac{1}{2}}. \tag{23}$$

Hence, from the above analysis, we anticipate that a first Hopf bifurcation will emerge close to $\beta_1 \simeq 1.2$, and lead to the emergence of a limit-cycle of frequency $\omega_1 \simeq 2\pi \times 5$ MHz, which correspond to T-periodic oscillations. Naturally, we expect that since the bifurcation point β_1 is defined as the threshold gain value to trigger the oscillations, the fixed point $(x_{\rm st}; y_{\rm st}) = (0; -\theta\beta\alpha)$ will be stable stable for $\beta < \beta_1$ and unstable beyond.

The second bifurcation point is obtained after considering the approximation $\tan(\omega_2 T) \simeq \omega_2 T$. From solving Eqs. (20) and (21), we find that the critical frequency and gain corresponding to that second Hopf bifurcation are

$$\omega_2 \simeq \frac{1}{\sqrt{\theta(T+\tau)}} \tag{24}$$

$$\beta_2 \simeq \left[1 + \frac{(T+\tau)}{\theta}\right]^{\frac{1}{2}}. \tag{25}$$

Therefore, when β is increased and reaches the value $\beta_2 \simeq 1.32$, the limit-cycle of frequency $\omega_2 \simeq 2\pi \times 612$ kHz emerges and becomes another stable attractor.

It therefore appears that the condition $I_{\rm pol} > I_{\rm th}$ is necessary for the emergence of an oscillatory behavior, and that depending on the gain, at least two different kinds of oscillations can be obtained. These analytical findings will be experimentally and numerically confirmed in the next section.

It is however interesting to note that in the case of very small delay ($T \ll \tau, \theta$), the exponential term in Eq. (17) can be set to 1 and in that case, the Hopf bifurcation condition $\lambda = i\omega$ yields the equations

$$\omega_0 \simeq \frac{1}{\sqrt{\theta\tau}} \tag{26}$$

$$\beta_0 \simeq 1. \tag{27}$$

Therefore, the oscillations are triggered for $\beta > 1$ and the frequency of the limit cycle is $\omega_0 = 2\pi \times 1.84$ MHz, which falls within the oscillator's bandwidth.

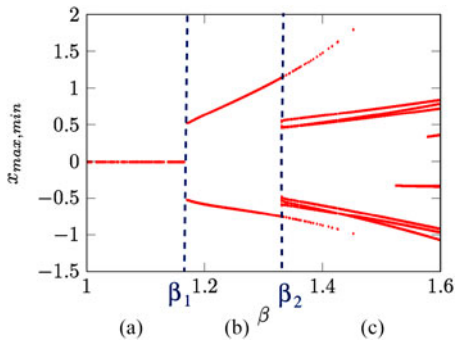

Fig. 2. Numerical bifurcation diagram, where the extrema of the variable x are plot as the gain β is increased. There are no oscillations in area (A), fast-scale oscillations in area (B), and slow-scale oscillations in area (C).

IV. Numerical and Experimental Results

A. Bifurcation Diagram

The full bifurcation behavior of the system is displayed in the bifurcation diagram of Fig. 2. The bifurcation diagram is obtained by plotting the maxima of the variable $x(t)$ as a function of the control parameter β. It synthetically represents the various dynamical states that can be obtained as the feedback gain of the system is varied. We have divided this numerical bifurcation diagram in three parts. The first part (A) is the region where $\beta < 1.18$, and where there are no oscillations in the system. The signal is null, the trivial fixed point is exponentially stable, and there is no other attractor in the system. The second area (B) is the region for which $1.18 < \beta < 1.34$, where the fast-scale limit-cycle oscillations of frequency ω_1 are sustained. The last area (C) is the region where $\beta > 1.34$, and where the slow-timescale limit-cycles of frequency ω_2 can be excited. The determination of the sub- or super-critical nature of these bifurcations remains an open point, and the bifurcation analysis would face the same difficulties that are encountered while investigating systems with nonlinear transfer functions that are piecewise linear (like in the Chua circuit for example).

B. Comparison Between Numerical and Experimental Results

The setup described in Fig. 1 has been used to record and analyze the oscillating waveforms. From the experimental viewpoint, the gain is varied through the control voltage $V_{\rm cr}$ of the VVA, while it is varied through β (which is proportional to G) for numerical simulations. The polarization voltage is taken as $V_{\rm th} - V_{\rm pol} = 0.5$ V in order to allow the laser to reach the region of linear increase (note that experimentally, the polarization voltages for the laser are negative in our setup). In Fig. 3, we have displayed the experimental timetraces along with the numerical ones obtained from the simulation of Eqs. (7) and (6). Fig. 3(a) and (d) illustrate the fast T-periodic oscillations, which are observed if $\beta \geq \beta_1$. This condition experimentally corresponds to $V_{\rm cr} \geq 26.6$ V. It is also interesting to note that these oscillations are asymmetric. Fig. 3(b) and (e) correspond to the situation observed when β is further increased and has passed the second bifurcation point β_2. This Hopf bifurcation leads to slow-scale oscillations of frequency ω_2. Subsequent increase of the gain

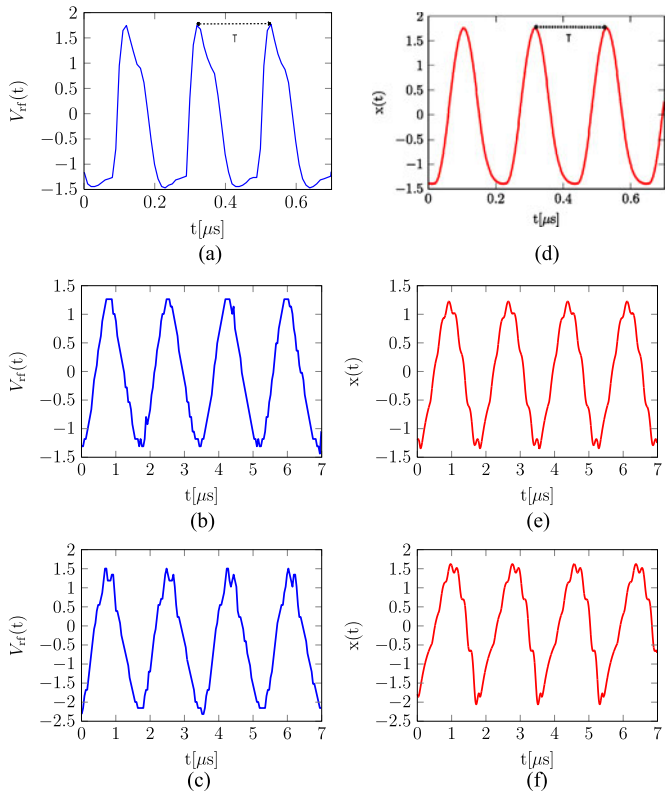

Fig. 3. Experimental (left column) and numerical (right column) timetraces of the OEO. For the experimental results we have set the polarization voltage at $V_{\rm pol} = -2.5$ V and the control voltage was set to (a) $V_{\rm cr} = 26.6$ V; (b) $V_{\rm cr} = 20.1$ V; (c) $V_{\rm cr} = 22.0$ V. For the numerical simulations of Eqs. (7) and (6) we have set $\alpha = -0.5$ and the feedback gain was set to (d) $\beta = 1.29$; (e) $\beta = 1.37$; (f) $\beta = 1.6$.

leads to the same kind of oscillations [see Figs. 3(c) and (f)], but with higher amplitude. It also appears that in the area (C), fast-scale T-periodic oscillations appear on top of this slow-scale limit-cycles, and give them a crenellated structure.

C. Discussion

It is interesting to compare the multi-scale dynamics investigated in this work with results that have been obtained previously in the context of OEOs with external Mach–Zehnder modulator. Indeed, the diode-nonlinear OEO has a sequence of bifurcations that shares many similarities and dissimilarities with the case of the classical (sine-nonlinear) OEO [19]–[21].

As far as similarities are concerned, we note that as for the conventional wideband OEOs, slow-time-scale oscillations can arise in the system when the gain is increased beyond a critical gain value which is always higher than 1 [11], [22]. The frequency in this slow-scale oscillation also depends in a non-trivial fashion on the three typical time constants of the system, namely τ, θ, and T. The critical values corresponding to these Hopf bifurcations depend on these three time constants as well.

On the other hand, the main dissimilarity is that the fixed-point structure is obviously different, and exclusively depends on how the LD is polarized. The fact the nonlinearity differs from the sine-function of conventional OEOs also leads to different values for the Hopf frequencies and critical gain points. It can also be noted that the timetraces are qualitatively very different: they display here a quasi-sinusoidal structure on top of which we can observe fast-scale oscillations, and this kind of multi-scale oscillations have never been observed so far in OEOs.

V. Conclusion

In this paper, we have investigated the simplest architecture of OEO, which is characterized by a piece-wise linear LD nonlinearity and a delayed feedback loop. We have built the experimental system and established the time-domain equations describing its dynamics. We showed that the bifurcation diagram exhibits a cascade of bifurcations, characterized by fast T-periodic oscillations after the first bifurcation, followed by a slow-scale limit-cycle which appears when the feedback gain increased. The theoretical study of the dynamics of our system critically depends on how the LD is polarized. We have compared the numerical simulations of our model with experimental measurements and we have found an excellent agreement between both sets of data.

This diode-nonlinear OEO represents a significant simplification with regards to the conventional sine-nonlinear OEO, and it has the potential to be an excellent benchmark for both fundamental and applied research in the topic of OEOs. For example, the dynamical properties of systems with piece-wise nonlinearity is a very active area for experimental and theoretical of research. The paradigmatic system in this area is the well known Chua circuit which is the focus of much interest for a wide spectrum of scientists, ranging from applied mathematicians to circuit design engineers. Hence, we believe that our OEO could contribute to a better understanding of this family of dynamical systems in particular, and of delayed autonomous oscillators in general [3], [23]–[25]. Future research will consider the exploration of the exact nature of the bifurcations presented in this work (sub-or super-critical), since the bifurcation diagram has clearly indicated that the emergence of the various bifurcations is non-trivial. We will also investigate in a future work the regime of high gain where hyperchaos is likely to arise. The main application of OEOs is ultra-stable microwave generation in the GHz-range, and it will also be interesting to investigate the stability (phase-noise performance and Allan deviation) of this diode-nonlinear OEO in these frequency ranges [26], [27]. As emphasized earlier, it should be noted that for a GHz oscillation, the internal dynamics of the laser might have to be considered because the microwave could excite the laser relaxation oscillations which are ruled by the intracavity internal photon and carrier dynamics [13]–[18], an therefore, the phase noise analysis is in that case an arduous task. Finally, we expect this oscillator to be an interesting alternative for many other potential applications, including from neuromorphic computing [28], oscillator synchronization [29], [30], or optical pulse generation [31].

Acknowledgment

G. R. Goune Chengui would like to thank S. T. Kingni from the University of Maroua, Cameroon, for valuable discussions about the bifurcation behavior of this system.

REFERENCES

[1] A. Neyer and E. Voges, "Dynamics of electrooptic bistable devices with delayed feedback," *IEEE J. Quantum Electron.*, vol. QE-18, no. 12, pp. 2009–2015, Dec. 1982.

[2] K. Ikeda, "Multiple-valued stationary state and its instability of the transmitted light by a ring cavity system," *Opt. Commun.*, vol. 30, pp. 257–261, 1979.

[3] L. Larger, "Complexity in electro-optic delay dynamics: Modeling, design, and applications," *Phil. Trans. R. Soc. A*, vol. 371, 20120464, 2013.

[4] X. S. Yao and L. Maleki, "High frequency optical subcarrier generator," *Electron. Lett.*, vol. 30, pp. 1525–1526, 1994.

[5] X. S. Yao and L. Maleki, "Optoelectronic microwave oscillator," *J. Opt. Soc. Am. B*, vol. 13, pp. 1725–1735, 1996.

[6] L. Maleki, "The optoelectronic oscillator," *Nature Photon.*, vol. 5, pp. 728–730, 2011.

[7] Y. K. Chembo, L. Larger, H. Tavernier, R. Bendoula, E. Rubiola, and P. Colet, "Dynamic instabilities generated with optoelectronic oscillators," *Opt. Lett.*, vol. 32, pp. 2571–2573, 2007.

[8] Y. K. Chembo, L. Larger, R. Bendoula, and P. Colet, "Effects of gain and bandwidth on the multimode behavior of optoelectronic microwave oscillators," *Opt. Exp.*, vol. 16, pp. 9067–9072, 2008.

[9] Y. K. Chembo, L. Larger, and P. Colet, "Nonlinear dynamics and spectral stability of optoelectronic microwave oscillators," *IEEE J. Quantum Electron.*, vol. 44, no. 9, pp. 858–866, Sep. 2008.

[10] J.-P. Goedgebuer, P. Levy, L. Larger, C.-C. Chen, and W. T. Rhodes, "Optical communication with synchronized hyperchaos generated electrooptically," *IEEE J. Quantum Electron.*, vol. 38, no. 9, pp. 1178–1183, Sep. 2002.

[11] Y. C. Kouomou, P. Colet, L. Larger, and N. Gastaud, "Chaotic breathers in delayed electro-optical systems," *Phys. Rev. Lett.*, vol. 95, 203903, 2005.

[12] B. Romeira, J. Javaloyes, J. M. L. Figueiredo, C. N. Ironside, H. I. Cantu, and A. E. Kelly, "Delayed feedback dynamics of Lienard-type resonant tunneling-photo-detector optoelectronic oscillators," *IEEE J. Quantum Electron.*, vol. 49, no. 1, pp. 31–42, Jan. 2013.

[13] G. Giacomelli, M. Calzavara, and F. T. Arecchi, "Instabilities in a semiconductor laser with delayed optoelectronic feedback," *Opt. Commun.*, vol. 74, pp. 97–101, 1989.

[14] S. Tang and J. M. Liu, "Chaotic pulsing and quasiperiodic route to chaos in a semiconductor laser with delayed opto-electronic feedback," *IEEE J. Quantum Electron.*, vol. 37, no. 3, pp. 329–336, Mar. 2001.

[15] H. D. I. Abarbanel, M. B. Kennel, L. Illing, S. Tang, H. F. Chen, and J. M. Liu, "Synchronization and communication using semiconductor lasers with optoelectronic feedback," *IEEE J. Quantum Electron.*, vol. 37, no. 10, pp. 1301–1311, Oct. 2001.

[16] F.-Y. Lin and J.-M. Liu, "Nonlinear dynamics of a semiconductor laser with delayed negative optoelectronic feedback," *IEEE J. Quantum Electron.*, vol. 39, no. 4, pp. 562–568, Apr. 2003.

[17] S. Tang, R. Vicente, M. C. Chiang, C. R. Mirasso, and J.-M. Liu, "Nonlinear dynamics of semiconductor lasers with mutual optoelectronic coupling," *IEEE J. Sel. Topics Quantum Electron.*, vol. 10, no. 5, pp. 936–943, Sep./Oct. 2004.

[18] G.-Q. Xia, S.-C. Chan, and J.-M. Liu, "Multistability in a semiconductor laser with optoelectronic feedback," *Opt. Exp.*, vol. 15, pp. 572–576, 2007.

[19] A. B. Cohen, B. Ravoori, T. E. Murphy, and R. Roy, "Using synchronization for prediction of high-dimensional chaotic dynamics," *Phys. Rev. Lett.*, vol. 101, 154102, 2008.

[20] K. E. Callan, L. Illing, Z. Gao, D. J. Gauthier, and E. Scholl, "Broadband chaos generated by an optoelectronic oscillator," *Phys. Rev. Lett.*, vol. 104, 113901, 2010.

[21] B. Ravoori, A. B. Cohen, J. Sun, A. E. Motter, T. E. Murphy, and R. Roy, "Robustness of optimal synchronization in real networks," *Phys. Rev. Lett.*, vol. 107, 034102, 2011.

[22] G. R. Goune Chengui, A. F. Talla, J. H. T. Mbe, A. Coillet, K. Saleh, L. Larger, P. Woafo, and Y. K. Chembo, "Theoretical and experimental study of slow-scale Hopf limit-cycles in laser-based wideband optoelectronic oscillators," *J. Opt. Soc. Am. B*, vol. 31, pp. 2310–2316, 2014.

[23] T. Erneux, *Applied Delay Differential Equations*. New York, NY, USA: Springer, 2010.

[24] M. Lakshamanan and D. V. Senthikumar, *Dynamics of Nonlinear Time-Delay Systems*. New York, NY, USA: Springer, 2011.

[25] M. C. Soriano, J. Garcia-Ojalvo, C. R. Mirasso, and I. Fischer, "Complex photonics: Dynamics and applications of delay-coupled semiconductors lasers," *Rev. Mod. Phys.*, vol. 85, 421–470, 2013.

[26] Y. K. Chembo, K. Volyanskiy, L. Larger, E. Rubiola, and P. Colet, "Determination of phase noise spectra in optoelectronic microwave oscillators: A langevin approach," *IEEE J. Quantum Electron*, vol. 45, no. 2, pp. 178–186, Feb. 2009.

[27] K. Volyanskiy, Y. K. Chembo, L. Larger, and E. Rubiola, "Contribution of laser frequency and power fluctuations to the microwave phase noise of optoelectronic oscillators," *J. Lightw. Technol.*, vol. 28, no. 18, pp. 2730–2735, Sep. 2010.

[28] R. Martinenghi, S. Rybalko, M. Jacquot, Y. K. Chembo, and L. Larger, "Photonic nonlinear transient computing with multiple-delay wavelength dynamics," *Phys. Rev. Lett.*, vol. 108, 244101, 2012.

[29] Y. C. Kouomou and P. Woafo, "Cluster synchronization in coupled chaotic semiconductor lasers and application to switching in chaos-secured communication networks," *Opt. Commun.*, vol. 223, no. 4, 283–293, 2003.

[30] Y. C. Kouomou and P. Woafo, "Generalized correlated states in a ring of coupled nonlinear oscillators with a local injection," *Phys. Rev. E*, vol. 66, 066201, 2002.

[31] Y. K. Chembo, A. Hmima, P.-A. Lacourt, L. Larger, and J. M. Dudley, "Generation of ultralow jitter optical pulses using optoelectronic oscillators with time-lens soliton-assisted compression," *J. Lightw. Technol.*, vol. 27, no. 22, pp. 5160–5167, Nov. 2009.

Géraud Russel Goune Chengui received the M.S. degree in physics from the University of Dschang, Dschang, Cameroon, in 2010. Since 2012, he has been working toward the Ph.D. degree at the University of Yaoundé, Yaoundé, Cameroon. He is investigating the multiscale nonlinear dynamics of optoelectronic oscillators.

Paul Woafo received the Ph.D. degree in physics from the University of Yaoundé, Yaoundé, Cameroon, in 1992, and the Doctorat d'Etat in physics in 1997. He his currently a Full Professor at the University of Yaoundé, and heads the Laboratory of Modelling and Simulation in Engineering, Biomimetics and Prototypes. He has published more than 180 refereed articles in international journals. He is a Founding Member and former President of the Cameroonian Physical Society, and a Vice-President of the African Physical Society. He was awarded the TWAS Prize for Young Scientists in 2004, and was a member of the International Union of Pure and Applied Physics commission for statistical physics (C3). He is currently a Senior Associate of the International Center for Theoretical Physics, and a Georg Forster Fellow of the Humboldt Foundation, Germany. His research interests involve the nonlinear and stochastic dynamics in optoelectronics, electromechanics, and biological systems.

Yanne K. Chembo (SM'12) received the Ph.D. degree in physics from the University of Yaoundé, Yaoundé, Cameroon, in 2005, and the Ph.D. degree in laser physics from the Institute for Cross-Disciplinary Physics and Complex Systems, Palma de Mallorca, Spain, in 2006. In 2007 and 2008, he was a Postdoctoral Fellow at the Franche-Comté Electronique, Mécanique, Thermique et Optique—Sciences et Technologies (FEMTO-ST) Institute, Besançon, France. In 2009, he was a NASA Postdoctoral Program Fellow at the Jet Propulsion Laboratory, Pasadena, CA, USA. Since 2010, he has been a Senior Research Scientist at the Centre National de la Recherche Scientifique, with affiliation at the FEMTO-ST Institute. He has published more than 100 articles in refereed international journals and conference proceedings. His research interests include microwave photonics, optoelectronics, complex systems, as well as applied nonlinear, stochastic, and quantum dynamics.